Impurity-induced magnetism in Pb$_{1-x-y}$Ge$_x$Yb$_y$Te

E. P. Skipetrov*

Low Temperature Physics Department, Moscow State University, 119899 Moscow, Russia

N. A. Chernova[†]

Department of Physics, Binghamton University, State University of New York, Binghamton, New York 13902-6016

E. I. Slyn'ko

Institute of Material Science Problems, Chernovtsy Department, 274001 Chernovtsy, Ukraine

We have studied the magnetic susceptibility and magnetization of the diluted magnetic semiconductor Pb$_{1-x-y}$Ge$_x$Yb$_y$Te. The susceptibility measured is a superposition of the matrix diamagnetism, the paramagnetic contribution of electrons localized in the ytterbium-band, and the Curie-Weiss paramagnetism provided by Yb^{3+} ions. The concentration of Yb^{3+} ions increases monotonically with the ytterbium content, while a significant fraction of ytterbium ions remains in a nonmagnetic Yb^{2+} state. This is explained within the electronic band-structure model, assuming the ytterbium-derived donor states form an impurity band in the vicinity of the valence-band top. In terms of this model the Yb^{3+} concentration and electronic population of the impurity band are determined as a function of the alloy composition.

I. INTRODUCTION

IV-VI semiconducting alloys containing magnetic impurities (Mn, Cr, Ce, Eu, Gd, Yb) form an important group of diluted magnetic semiconductors, which have attracted much attention due to the effects arising from the interaction between charge carriers and local magnetic moments.[1-6] These are, for example, carrier-concentration-induced magnetic phase transitions in Mn-based alloys, resonant enhancement of $f-f$ exchange in Sn$_{1-x}$Gd$_x$Te ($x<0.05$) at certain hole concentrations, and the switch of the chromium magnetic activity under variation of the composition in Pb$_{1-x}$Sn$_x$Te:Cr. The key point of these effects is that they are caused by a shift of the Fermi level with respect to either electronic band edges of the host semiconductor or $d(f)$-derived impurity bands.

Among the magnetic impurities listed above, ytterbium is the only one whose atom has a completely filled internal electronic shell ($4f^{14}5s^25p^66s^2$). One can expect a nonmagnetic Yb^{2+} ($4f^{14}5s^25p^6$) charge state from this impurity in a crystal lattice of IV-VI alloys. Nevertheless, magnetic Yb^{3+} ($4f^{13}5s^25p^6$) ions have been revealed in Pb$_{1-x}$Yb$_x$Te, Pb$_{1-x}$Yb$_x$Se, and Pb$_{1-x}$Yb$_x$S by electron paramagnetic resonance.[7] It has also been found that in Pb$_{1-x-y}$Ge$_x$Yb$_y$Te the electronic band of $4f$-derived states is situated in the vicinity of the valence-band top, and the Fermi level is pinned at the $4f$ band.[6,8] The impurity band energy depends strongly upon the alloy composition, temperature, and pressure—variation of these parameters results in a shift of the impurity band with respect to the valence-band edge: from resonant with the valence-band continuum to localization in the gap. However, no correlation between the impurity band energy and the magnetic activity of ytterbium has been established so far.

Therefore, the goal of this study is to examine the magnetic ion concentration in Pb$_{1-x-y}$Ge$_x$Yb$_y$Te of various compositions. We suppose that a variation of Ge and Yb molar fractions would allow us to shift the impurity band energy with respect to the valence-band edge, as both impurities are well known to increase the energy gap in the alloys.[9,10] In addition, a variation of the Yb content should also change the total number of states in the impurity band and may affect the magnetic ion concentration in the alloys.

II. EXPERIMENT

Two single-crystal ingots were grown for the present experiments by the Bridgman method.[11] The component ratios in the pregrowth charges were the following: Pb$_{1-y}$Yb$_y$Te ($y=0.015$) and Pb$_{1-x-y}$Ge$_x$Yb$_y$Te ($x=0.1,y=0.005$). The cylindrical ingots grown were cut into thin disks, in which the ytterbium and germanium concentrations were checked by an energy-dispersive x-ray fluorescence analysis. It was found that the ytterbium concentration C_{Yb} attains its maximum at the origin, exponentially decreasing along the ingots. The germanium concentration was measured to be quite uniform all over the original part of the Pb$_{1-x-y}$Ge$_x$Yb$_y$Te ingot, $C_{\text{Ge}}\approx2$ mol.%, while there was a sharp increase of C_{Ge} at the end part. The samples for galvanomagnetic and magnetic studies were made from each representative disk, for sample parameters, see Table I.

For sample preparation, each disk was cleaved in liquid nitrogen into bars with faces oriented along ⟨100⟩ directions. For the magnetic measurements, combined samples made of these bars of the total weight 0.7–0.8 g were glued onto the plastic holder. In each sample the temperature and magnetic-field dependences of the magnetization were measured using a vibrating sample magnetometer EG & G PARC M155, detecting the magnetic moment down to 5×10^{-5} emu. Measurements were taken from room temperature to 5 K, in a magnetic field up to 0.5 T. The magnetic field was produced by an electromagnet and determined by means of Hall

TABLE I. Parameters of the investigated samples $Pb_{1-x-y}Ge_xYb_yTe$.

Sample	x	y	N_{Yb}, cm^{-3}	p, cm^{-3} at 4.2 K	$N_{Yb^{3+}}$, cm^{-3}	$N_{Yb^{3+}}/N_{Yb}$
1	0	0.0003	4.4×10^{18}	2.33×10^{18}	—	—
2	0	0.005	8.0×10^{19}	1.29×10^{17}	1.1×10^{19}	0.14
3	0	0.008	1.2×10^{20}	3.60×10^{16}	1.7×10^{19}	0.13
4	0	0.015	2.2×10^{20}	1.78×10^{16}	2.4×10^{19}	0.11
5	0	0.030	4.6×10^{20}	4.67×10^{15}	6.6×10^{19}	0.14
6	0	0.065	9.6×10^{20}	—	8.4×10^{19}	0.09
7	0.02	0.007	1.0×10^{20}	—	9.7×10^{18}	0.09
8	0.02	0.010	1.5×10^{20}	—	2.4×10^{19}	0.16
9	0.02	0.014	2.1×10^{20}	—	3.7×10^{19}	0.18
10	0.02	0.019	2.8×10^{20}	—	7.6×10^{19}	0.27

probes. For the temperature variation a liquid helium gas-flow cryostat equipped with a heater was used. Temperature was controlled by a calibrated Cu-CuFe thermocouple, whose cold end was glued onto the sample face and the hot one was immersed into a melting ice.

For the galvanomagnetic study, small bars ($1 \times 1 \times 5$ mm^3) cleaved from each representative disk were used. Voltage and Hall contacts made of platinum wire were welded onto the sides of the sample using a spark discharger. Copper current wires were attached to the sample using the alloy of In with 4% Ag and 1% Au. In each sample the Hall coefficient and the resistivity at 4.2 K were measured. All the samples revealed a p-type conductivity; the hole concentration obtained from the Hall coefficient is presented in Table I.

III. RESULTS AND DISCUSSION

A. Paramagnetic susceptibility of ytterbium-band electrons

The magnetic susceptibility χ measured reveals a competition between the diamagnetic and paramagnetic contributions (Fig. 1). Let us, first, analyze in detail the diamagnetic part χ_0, gaining at a high temperature. It appears to be temperature independent, so we determined the χ_0 values from a saturation level of $\chi(T)$ curves at $T \approx 250$ K. The diamagnetic contribution is usually connected to a diamagnetism of the host semiconductor lattice. We have also found good agreement in χ_0 values determined by us for very diluted $Pb_{1-y}Yb_yTe$ and the values known for lead telluride.[12,13] The most interesting result observed is a monotonic reduction of the diamagnetic contribution (here we mean its absolute value) with increasing Yb molar fraction. This reveals a paramagnetic susceptibility significant even at high temperature and growing with ytterbium content. In rather diluted $Pb_{1-y}Yb_yTe$ a rapid, close to linear, growth of this paramagnetism occurs, followed by a slower increase at higher Yb content (see the inset in Fig. 1).

We attribute this paramagnetic contribution to the electrons trapped in the impurity band, in analogy with one observed earlier in lead telluride doped with thallium or in tin telluride doped with indium, similar to conditions of the Fermi level being pinned at the energy of the impurity states situated in the valence band.[14,15] In this case an additional

paramagnetic contribution to the magnetic susceptibility should be controlled by the density of states at the Fermi level located within the impurity band. In order to confirm this hypothesis, we estimate the susceptibility of such electrons theoretically, using the approach introduced in Ref. 16. The electrons in an impurity band, being free to move through the whole crystal, form a Fermi gas, whose spin susceptibility is given by

$$\chi = \mu_B^2 \frac{\partial n_{Yb}}{\partial \varepsilon_F}, \tag{1}$$

where μ_B is the Bohr magneton, n_{Yb} is the electron population of impurity band, and ε_F is the Fermi energy. As pointed out earlier, the Fermi level is pinned at the energy of the impurity states in the alloys considered. Thus, in the low-temperature limit, a number of trapped electrons can be defined as
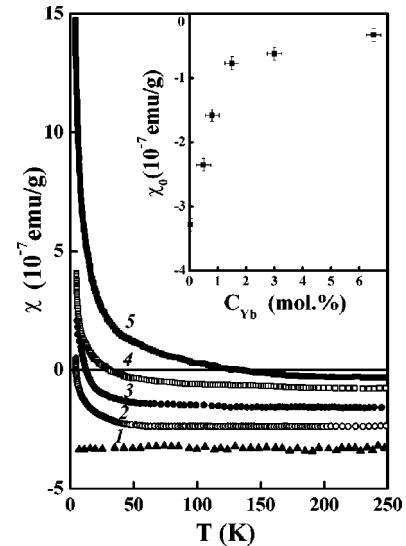

FIG. 1. Temperature dependence of the magnetic susceptibility in $Pb_{1-y}Yb_yTe$ alloys of various ytterbium content y: (1) 0.0003, (2) 0.005, (3) 0.008, (4) 0.015, and (5) 0.065. The inset presents the high-temperature diamagnetic contribution as a function of ytterbium content.
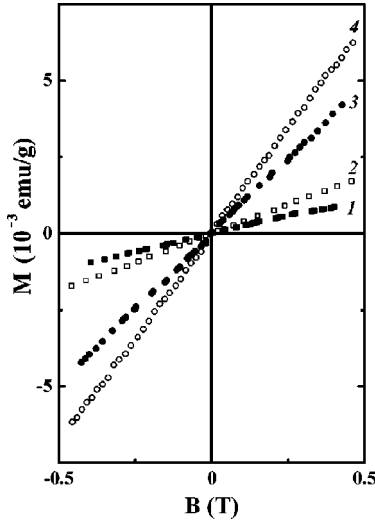
FIG. 2. Magnetization of Pb$_{1-x-y}$Ge$_x$Yb$_y$Te alloys at 5 K. (1) $x=0.02$, $y=0.01$; (2) $x=0$, $y=0.015$; (3) $x=0.02$, $y=0.019$; (4) $x=0$, $y=0.065$.

FIG. 3. Reverse magnetic susceptibility corrected due to the diamagnetic share as a function of temperature for Pb$_{1-x-y}$Ge$_x$Yb$_y$Te ($x=0.02$) alloys. (1) $y=0.007$, (2) $y=0.010$, (3) $y=0.014$, and (4) $y=0.019$.

$$n_{Yb} = \int_{-\infty}^{\varepsilon_F} g_{Yb}(\varepsilon) d\varepsilon, \qquad (2)$$

where $g_{Yb}(\varepsilon)$ denotes the density of states in the ytterbium band. Combining Eqs. (1) and (2), we find

$$\chi = \mu_B^2 g_{Yb}(\varepsilon_F). \qquad (3)$$

Estimations of $g_{Yb}(\varepsilon_F)$ from Eq. (3) show that density of states in the impurity band increases from 1.6×10^{19} to 4.7×10^{19} cm^{-3} meV^{-1} with the ytterbium content. The density of impurity states might also be estimated by dividing the total number of the impurity states (see column 4 in Table I) by the energy width of the impurity band. The latter was estimated by us earlier as 5–10 meV.[8] This method yields the density of impurity states on the order of 10^{19} cm^{-3} meV^{-1}, which is in a good agreement with the one obtained from magnetic measurements.

B. Low-temperature paramagnetism and concentration of Yb^{3+} ions

The paramagnetic susceptibility becomes dominating at a low temperature, when its rapid Curie-like growth occurs (Fig. 1). The low-field magnetization curves measured at 5 K are linear, which is typical for the paramagnets (Fig. 2). A reciprocal paramagnetic contribution $1/(\chi-\chi_0)$ increases linearly with temperature (Fig. 3), that allows one to determine the Curie temperature and Curie constant for the alloys of various Yb and Ge content as follows from the Curie-Weiss law:

$$\chi - \chi_0 = \frac{C}{T-\Theta}, \qquad (4)$$

where C and Θ are the Curie constant and temperature, respectively. The subtracted diamagnetic part χ_0 is the one plotted in Fig. 1 (inset), individual for each alloy composition.
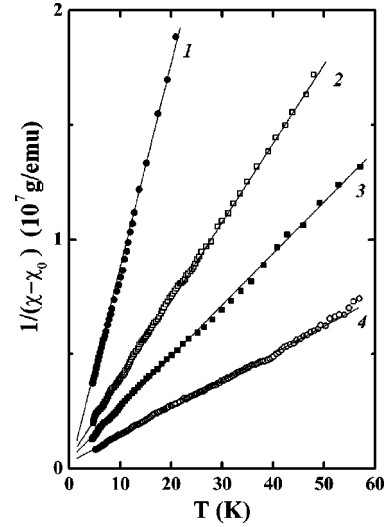
The experimental $1/(\chi-\chi_0)$ curves intersect the abscissa at slightly negative temperature $\Theta = -1$–2 K, indicating a rather weak antiferromagnetic exchange between the magnetic centers. The concentration of Yb^{3+} single ions $N_{Yb^{3+}}$ were then calculated from the Curie constants:

$$N_{Yb^{3+}} = \frac{3k_B C}{g^2 \mu_B^2 S(S+1)}. \qquad (5)$$

Here k_B is the Boltzmann constant; g and S are the g factor and effective spin of the ground electronic state, respectively. The parameters of the Yb^{3+} ground state in lead telluride, $g=2.52$ and $S=1/2$, we used were experimentally determined by electron paramagnetic resonance in Ref. 7.

The magnetic ion concentration in the alloys is presented in Table I, together with the total ytterbium content N_{Yb} computed from x-ray analysis data. Comparison of these data sets reveals only 10–15 % of magnetic ions in Pb$_{1-y}$Yb$_y$Te, independent of the total ytterbium content there. A different situation is observed in Ge doped alloys, where an increase of the Yb content leads to a pronounced growth of the magnetic Yb^{3+} ion fraction. Remarkably, in all the investigated alloys, the concentration of magnetic ions increases with ytterbium content.

C. Magnetic ion emergence and electronic band structure

For the sake of a clear understanding of the origin of magnetic ion in Pb$_{1-x-y}$Ge$_x$Yb$_y$Te, let us refer to the charge-carrier energy spectrum in these alloys (Fig. 4). In Pb$_{1-x}$Ge$_x$Te the free-carrier concentration is determined by electrically active native point defects of several types.[17] The dominating type of defects, metal vacancies, provides the acceptor levels; as a result, the Fermi level stays in the valence band, and a free hole concentration is determined by an effective concentration of the native point acceptors N_i^* (left
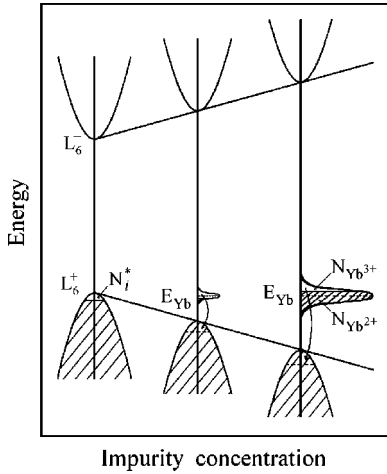
FIG. 4. Variation of the energy spectrum with an increase of Yb concentration in $Pb_{1-x-y}Ge_xYb_yTe$.

FIG. 5. Concentration of magnetic Yb^{3+} ions as a function of ytterbium content in $Pb_{1-y}Yb_yTe$ (solid squares) and $Pb_{1-x-y}Ge_xYb_yTe$ (open circles). Curve (1) shows the dependence in the case of a constant concentration of native defects. Curves (2) and (3) correspond to linear [Eq. (7)] and quadratic [Eq. (8)] increases of the native defect concentration, respectively.

section in Fig. 4). Ytterbium doping introduces a donor impurity band right above the valence-band top.[8] A fraction of electrons transfers from the impurity band to the empty states in the valence band, and the Fermi level becomes pinned at the energy of the impurity states (middle section in Fig. 4). By this redistribution of electrons, a fraction of ytterbium ions transfer from the Yb^{2+} charge state (nonmagnetic) to the Yb^{3+} (magnetic) state. Thus, if the impurity band is situated above the valence-band edge, the concentration of magnetic ions should be exactly equal to the concentration of the empty electronic states in the valence band, arising from the native point defects.

As follows from Table I, the magnetic ion concentration in $Pb_{1-x-y}Ge_xYb_yTe$ increases with Yb content, and so should the native point defect concentration, as these defects are the only candidates to accept the electrons from Yb ions. This effect, usually referred to as self-compensation, is known for many other doped IV-VI semiconductors: to the benefit of the total electronic energy of a crystal the native acceptors are formed to compensate partially for the donor effect of doping.[17] The rate of native defect formation in $Pb_{1-x-y}Ge_xYb_yTe$ is significantly less than the increment of the ytterbium content with doping. As a result, at a high enough ytterbium content, most of the impurity ions are in Yb^{2+} state and the impurity band is almost filled with electrons (right section in Fig. 4).

The experimental dependence $N_{Yb^{3+}}(N_{Yb})$ (Fig. 5) allows us to characterize the kinetics of magnetic ion formation numerically, and to compute the electronic population of the impurity band in alloys of various ytterbium and germanium contents. According to the model introduced, the magnetic ion concentration can be expressed as a sum of two contributions:

$$N_{Yb^{3+}}=N_{i0}^*+f(N_{Yb}).\tag{6}$$

The first one, N_{i0}^*, denotes the effective concentration of native defects in undoped alloys; it accounts for the fraction of magnetic ions arising due to the original stock of native defects. The second part, $f(N_{Yb})$, is a concentration of native
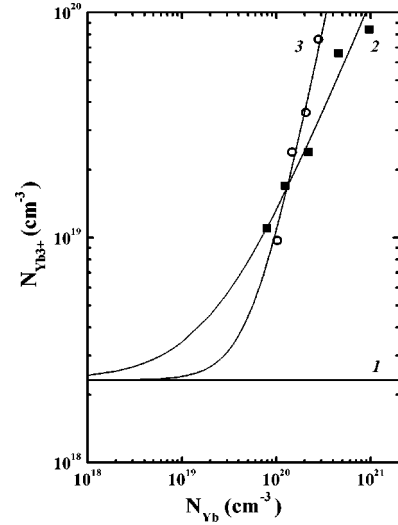
defects (and magnetic ions) as a function of the ytterbium concentration; it describes the formation of additional native defects with doping.

In order to define function $f(N_{Yb})$, we set N_{i0}^* equal to the free hole concentration in $Pb_{1-y}Yb_yTe$ with minimal ytterbium content (sample 1 in Table I). The corresponding constant concentration of magnetic ions is presented in Fig. 5 (curve 1). The experimental concentration of magnetic ions as a function of ytterbium concentration, plotted in Fig. 5, reveals $f(N_{Yb})$ as a power function. The exponent, determined as a slope of dependence on a double logarithmic scale, is very close to one in case of $Pb_{1-y}Yb_yTe$ and is accurately equal to 2 in the case of $Pb_{1-x-y}Ge_xYb_yTe$. We obtained the best fit (solid curves in Fig. 5) using functions

$$N_{Yb^{3+}}=2.3\times10^{18}+0.11N_{Yb},\tag{7}$$

$$N_{Yb^{3+}}=2.3\times10^{18}+8.5\times10^{-22}N_{Yb}^2\tag{8}$$

for $Pb_{1-y}Yb_yTe$ and $Pb_{1-x-y}Ge_xYb_yTe$, respectively.

Using approximations (7) and (8), a dependence of electronic population of the impurity band was computed (Fig. 6). In spite of the experimental values (expressed as a ratio of filled impurity states to the total capacity of the impurity band) are mostly gathered in a narrow range of 0.8–0.9, the approximations (solid curves) exhibit different behaviors. In an imaginary case of a constant concentration of native defects (curve 1), the electronic population of the impurity band would grow from zero and tend to unity with the ytterbium content. If the native defect concentration grows linearly, as in $Pb_{1-y}Yb_yTe$ (curve 2), the electronic population increases and comes to saturation at a certain value determined by the rate of defect formation [coefficient in Eq. (7)]. In the case of a quadratic increase of the defect concentration ($Pb_{1-x-y}Ge_xYb_yTe$, curve 3), the electronic population of
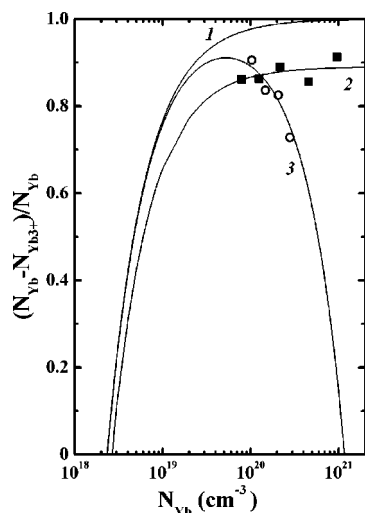
FIG. 6. Electron population of the Yb impurity band as a function of ytterbium content in Pb$_{1-y}$Yb$_y$Te (solid squares) and Pb$_{1-x-y}$Ge$_x$Yb$_y$Te (open circles). Curve (1) shows the dependence in the case of a constant concentration of native defects. Curves (2) and (3) correspond to linear [Eq. (7)] and quadratic [Eq. (8)] increases of the native defect concentration, respectively.

the impurity band increases, attains its maximum, and then drops to zero. This happens because at a high enough ytterbium content there are more native defects than impurity atoms in the alloys. Thus, for Pb$_{1-x-y}$Ge$_x$Yb$_y$Te, any fraction of occupied impurity states is possible.

IV. CONCLUSIONS

Ytterbium impurity brings two contributions to the magnetic susceptibility of Pb$_{1-x-y}$Ge$_x$Yb$_y$Te alloys: a temperature-independent paramagnetic contribution, attributed to a huge concentration of electrons in the Yb-derived band, and a Curie-Weiss paramagnetic contribution arising due to the magnetic Yb^{3+} ions.

In terms of the Curie-Weiss law, the concentration of magnetically active Yb^{3+} ions and the Curie temperature in Pb$_{1-x-y}$Ge$_x$Yb$_y$Te have been determined. It is shown that the concentration of magnetic ions increases with the ytterbium content, whereas a significant quantity of ytterbium remains in a nonmagnetic Yb^{2+} state.

The kinetics of magnetic ion formation with doping has been analyzed. In Pb$_{1-y}$Yb$_y$Te the concentration of magnetic ions increases linearly with the ytterbium concentration, while in Pb$_{1-x-y}$Ge$_x$Yb$_y$Te alloys it follows a quadratic function. Based on this result, the electronic population of the impurity level as a function of ytterbium content has been established.

*Electronic address: skip@mig.phys.msu.su

†On leave from: Low Temperature Physics Department, Moscow State University, 119899 Moscow, Russia.

[1] T. Story, G. Karczewski, L. Swierkowski, and R.R. Galazka, Phys. Rev. B **42**, 10477 (1990); T. Story, R.R. Galazka, R.B. Frankel, and P.A. Wolff, Phys. Rev. Lett. **56**, 777 (1986).

[2] T. Story, Z. Wilamowski, E. Grodzicka, B. Witkowska, and W. Dobrowolski, Acta Phys. Pol. A **84**, 773 (1993); W. Mac, T. Story, and A. Twardowski, *ibid.* **87**, 492 (1995).

[3] X. Gratens, S. Charar, M. Averous, S. Isber, J. Deportes, and Z. Golacki, Phys. Rev. B **56**, 8199 (1997).

[4] G. Bauer and H. Pascher, in *Diluted Magnetic Semiconductors*, edited by M. Jain (World Scientific, Singapore, 1991); R. Denecke, L. Ley, G. Springholz, and G. Bauer, Phys. Rev. B **53**, 4534 (1996).

[5] T. Story, M. Gorska, A. Lusakowski, M. Arciszewska, W. Dobrowolski, E. Grodzicka, Z. Golacki, and R.R. Galazka, Phys. Rev. Lett. **77**, 3447 (1996).

[6] E. Grodzicka, W. Dobrowolski, T. Story, E.I. Slynko, Yu.K. Vygranenko, M.M.H. Willekens, H.J.M. Swagten, and W.J.M. de Jonge, Acta Phys. Pol. A **90**, 801 (1996).

[7] S. Isber, S. Charar, X. Gratens, C. Fau, M. Averous, S.K. Misra, and Z. Golacki, Phys. Rev. B **54**, 7634 (1996).

[8] E.P. Skipetrov, N.A. Chernova, E.I. Slyn'ko, and Yu.K. Vygranenko, Phys. Rev. B **59**, 12 928 (1999).

[9] G.A. Antcliffe, S.G. Parker, and R.T. Bate, Appl. Phys. Lett. **21**, 505 (1972).

[10] S.K. Das and R. Suryanarayanan, J. Appl. Phys. **66**, 4843 (1989).

[11] Yu.K. Vygranenko, V.E. Slyn'ko, and E.I. Slyn'ko, Neorg. Mater. **31**, 1338 (1995) [Inorg. Mater. (Transl. of Neorg. Mater.) **31**, 1219 (1995)].

[12] M. Gorska and J.R. Anderson, Phys. Rev. B **38**, 9120 (1988).

[13] L.A. Fal'kovskii, A.V. Brodovoi, and G.V. Lashkarev, Zh. Éksp. Teor. Fiz. **80**, 334 (1981) [Sov. Phys. JETP **53**, 170 (1981)].

[14] K.I. Andronik, M.P. Boiko, and A.V. Luzhkovskii, Fiz. Tekh. Poluprovodn. **22**, 1878 (1988) [Sov. Phys. Semicond. **22**, 1190 (1988)].

[15] V.I. Kaidanov, S.A. Nemov, and Yu.I. Ravich, Fiz. Tekh. Poluprovodn. **26**, 201 (1992) [Sov. Phys. Semicond. **26**, 113 (1992)].

[16] E. Mooser, Phys. Rev. **100**, 1589 (1955).

[17] V.I. Kaidanov, S.A. Nemov, and Yu.I. Ravich, Fiz. Tekh. Poluprovodn. **28**, 369 (1994) [Semiconductors **28**, 223 (1994)].